Inositol Phosphorlyceramide Synthase null *Leishmania major* (Δ*ipcs*$^-$) are viable and virulent in animal infections where salvage of host sphingomyelin predominates

F. Matthew Kuhlmann[1,2], Phillip Key[1], Suzanne Hickerson[1], John Turk[2], Fong-Fu Hsu[2], and Stephen M. Beverley[1,*]

[1] Department of Molecular Microbiology, and [2] Department of Internal Medicine, Washington University School of Medicine, 660 S. Euclid Ave., Saint Louis, MO 63110, USA.

*Corresponding author: Stephen M. Beverley, Department of Molecular Microbiology, Box 8230, Washington University School of Medicine, 660 S. Euclid Ave., Saint Louis, MO 63110, USA. Tel: 314-747-2630, Fax: 314-747-2634; E-mail: stephen.beverley@wustl.edu

Keywords: Trypanosomatid protozoan parasite; Sphingolipids, inositol phorphorylceramide, lipid remodeling, lipid salvage, infectivity and virulence.

Running Title: *Leishmania* Null IPCS mutants are unexpectedly viable and virulent

Abstract.

Many pathogens synthesize inositolphosphorylceramide (IPC) as the major sphingolipid (SL), unlike the mammalian host where sphingomyelin or more complex SLs predominate. Thus, divergence between IPCS and mammalian sphingolipid synthases has prompted interest as a potential drug target. However, in the trypanosomatid protozoan *Leishmania*, promastigotes lacking *de novo* sphingolipid synthesis (Δ*spt2*-) survive and remain virulent, as amastigotes salvage host sphingolipids and are still able to produce IPC. To further understand the role of IPC, we generated null IPCS mutants in *L. major* (Δ*ipcs*$^-$). Unexpectedly and unlike fungi where IPCS is essential, Δ*ipcs*$^-$ was remarkably normal in culture and highly virulent in mouse infections. Both IPCS activity and IPC itself were absent in Δ*ipcs*$^-$ promastigotes and amastigotes, arguing against an alternative route of IPC synthesis. Notably, salvaged mammalian sphingomyelin was highly abundant in purified amastigotes from both WT and Δ*ipcs*$^-$. Quantitative estimation showed SM to be about 5-fold more abundant than IPC in WT, suggesting that normally SM is the dominant amastigote SL. Analysis of the WT amastigote IPC ceramide anchor showed that it arose not from *de novo* synthesis by the parasite, but through catabolism of mammalian SLs, probably through the action of the parasite sphingomyelinase *ISCL*. These data suggest that SM salvage may account for the survival and virulence of Δ*ipcs*$^-$, a finding which likely mitigates the suitability of IPCS as a chemotherapeutic target.

Introduction.

Leishmaniasis is often considered a neglected tropical disease. Currently it is estimated that there are more than 1.7 billion people at risk and nearly 12 million people with symptomatic disease, ranging from mild cutaneous infections to severe disfiguring or lethal forms, with upwards of 50,000 deaths annually (Herwaldt 1999, Banuls, Bastien et al. 2011, Alvar, Velez et al. 2012, Pigott, Bhatt et al. 2014). Remarkably, the great majority of infections are undiagnosed and/or asymptomatic, suggesting that well more than 100 million people may harbor parasites (Banuls, Bastien et al. 2011, Mannan, Elhadad et al. 2021). Persistent asymptomatic infections constitute a double edged sword – while serving as a reservoir for transmission and/or reactivation, persistent parasites are known to mediate strong protective concomitant immunity against disease pathology (WHO 2010

, Banuls, Bastien et al. 2011, Singh, Hasker et al. 2014, Mannan, Elhadad et al. 2021). *Leishmania* have two distinct growth stages, a promastigote stage in the sand fly vector, and an intracellular amastigote stage residing within cellular endocytic pathways in the mammalian host (Herwaldt 1999). While the promastigote stage is readily cultured in the laboratory and amenable to molecular techniques, amastigotes require the use of macrophage infection systems or infections of animal models replicating key aspects of human disease.

While progress has been achieved in new chemotherapeutic strategies, many are not yet implemented clinically and resistance to several promising agents has already been observed (Croft, Sundar et al. 2006, den Boer, Argaw et al. 2011, Sangshetti, Khan et al. 2015), One pathway potentially offering important drug target is that of

sphingolipid synthesis (Zhang, Bangs et al. 2010, Guan and Maser 2017, Mina and Denny 2018). Sphingolipids (SL) are a diverse class of lipids that function in apoptosis, cell signaling, and membrane structure and these pathways have been targeted for therapies against a wide range of diseases including cancer, multiple sclerosis, and infectious diseases (Suzuki, Tanaka et al. 2008, Cohen, Barkhof et al. 2010, Oskouian and Saba 2010, Koeller and Heise 2011, Megyeri, Riezman et al. 2016, Hannun and Obeid 2018) . Sphingolipids differ in the nature of the head groups as well as the composition of the hydrophobic ceramide anchor, in different tissues and species, Unlike mammalian cells that primarily synthesize sphingomyelin (SM) and complex glycosphingolipids, *Leishmania* synthesize inositol phosphorylceramide (IPC) as their primary sphingolipid (Kaneshiro, Jayasimhulu et al. 1986), as do other protozoa, fungi and plants (Zhang, Bangs et al. 2010) (Harrison, Dunn et al. 2018).

This divergence has prompted scrutiny of IPCS as a drug target, where in fungi it is essential and repression causes decreased growth and virulence along with increased susceptibility to acidic environments (Heidler and Radding 2000, Luberto, Toffaletti et al. 2001). IPC is formed when Inositol Phosphorylceramide Synthase (IPCS) converts ceramide and phophatidylinositol to IPC and diacylglycerol (DAG). The related trypanosomatid parasite *Trypanosoma brucei* encodes four sphingolipid synthases (SLS), collectively mediating synthesis of sphingomyelin (SM), ethanolamine phosphorylceramide and IPC; inducible RNAi knockdowns of the entire locus were lethal, although the contribution of the individual genes/activities was not further dissected (Sutterwala, Hsu et al. 2008). *Leishmania* IPC Synthase has been pursued as a drug target by analogy of findings from pathogenic fungi as well as its divergence from

mammalian sphingomyelin synthases (Denny, Shams-Eldin et al. 2006). While aureobasidin A, a known inhibitor of yeast IPCS, was inactive against *Leishmania* and *Trypanasoma cruzi* (Sevova, Goren et al. 2010), other studies have revealed candidate inhibitors (Figueiredo, Dias et al. 2005, Mina, Mosely et al. 2010, Sevova, Goren et al. 2010, Mina, Mosely et al. 2011, Norcliffe, Mina et al. 2018).

Thus a biological requirement for *Leishmania* IPCS has not been addressed *in vivo*. That *Leishmania* could differ from other organisms was first suggested by the fact that *L. major* null mutants lacking the first enzyme in *de novo* sphingolipid synthesis, serine palmitoyl transferase (Δ*spt2*$^-$) completely lacked all SLs, yet remain viable in log phase culture (Zhang, Showalter et al. 2003, Denny, Goulding et al. 2004). Subsequent studies in promastigotes showed that sphingolipid catabolism was used to generate ethanolamine (EtN), whose provision to Δ*spt2*$^-$ parasites rescued a defect in differentiation to infective metacyclic parasites (Zhang, Pompey et al. 2007). While Δ*spt2*$^-$ was fully infective in animal models, it continued to synthesize IPC, presumably by salvage of potential precursor sphingolipid components from the host cell (Winter, Fuchs et al. 1994, Zhang, Hsu et al. 2005, Ali, Harding et al. 2011). Several routes could be envisaged; sphingoid bases or ceramide precursors could be salvaged directly, or mammalian sphingolipids could be acquired and catabolized for resynthesis as IPC sphingolipids. As all routes ultimately require IPCS for parasite IPC synthesis, we sought to generate Δ*ipcs*$^-$ null mutants if possible, and to explore their impact on IPC synthesis and/or metabolism, and virulence in animal models. Surprisingly, our data show convincingly *IPCS* was not essential, with SM salvage in WT cells rendering it the dominant amastigote SL as well as serving as the source of amastigote IPC. These

findings account for the dispensability of IPCS in animal infections, potentially dampening enthusiasm for IPCS as a useful drug target in this parasite,

Results

Targeted Replacement of *L. major IPCS*. The *L. major* genome is primarily diploid albeit with occasional aneuploidy, and typically two rounds of gene replacement are required to generate null mutants of single copy genes (Cruz, Coburn et al. 1991). Targeting constructs containing resistance markers to G418 (*NEO)* or nourseothricin (*SAT*) were designed to successively replace the *IPCS* ORF precisely by homologous gene replacement (Fig. 1A). To alleviate concerns about lethality of IPCS deficiency, we focused on the culturable promastigote stage where SLs are not required in any capacity in the presence of ethanolamine (Zhang, Showalter et al. 2003, Denny, Goulding et al. 2004, Zhang, Pompey et al. 2007). A secondary effect of IPCS deficiency could be ceramide accumulation which can be toxic (Hannun and Obeid 2002), and we also performed transfections in the presence of myriocin (an inhibitor of *de novo* SL synthesis) to potentially ameliorate this.

Heterozygous (*IPCS/IPCS::ΔNEO*) and homozygous null mutants (*IPCS*::Δ*SAT*/*IPCS*::Δ*NEO*; referred to as *Δipcs*$^-$) were readily obtained and confirmed by PCR tests to lack the IPCS coding region, accompanied by the expected planned replacements (analysis of the double homozygous replacement is shown in Fig. 1B). An episomal expression vector (pXG-BSD-IPCS) was used to restore *IPCS* expression, yielding the line *Δipcs*$^-$*/+IPCS* (Fig. 1 A,B). The recovery of *Δipcs*$^-$ clonal lines was readily accomplished with good efficiencies, regardless of EtN or myriocin treatment,

and these showed no obvious growth defects. Numerous transfectant lines were obtained and authenticated with similar phenotypes, and in this work results from one representative set of KO and IPCS-restored pair are shown.

IPCS activity is lost in *Δipcs*⁻ promastigotes. Enzymatic assays with promastigote microsomes were performed by evaluating the conversion of phosphatidylinositol (PtI) and NBD-Ceramide to NBD-IPC, after TLC separation, and quantitative fluoroscopy (Figs. 2A, S1A). High levels of NBD-IPC were generated in complete reactions bearing microsomes, NBD-Cer and PtI; this product was sensitive to PI-PLC digestion as expected. We purified and confirmed the presumptive NBD-IPC from the TLC plate by mass spectrometry[1]. Consistent with prior studies, aureobasidin A did not inhibit the *in vitro* reaction (Sevova, Goren et al. 2010). Little or no product was obtained if PtI or NBD-Cer were omitted, if PtC replaced PtI, or if microsomes were omitted or previously heat inactivated. These data confirmed our ability to assay IPCS, yielding the expected enzymatic properties (Figs. 2A, S2A).

We compared the IPCS activity of WT, *Δipcs*⁻/+ or *Δipcs*⁻/+ *IPCS* parasite mcirosomes (Figs. 2B, S1B). As expected, *Δipcs*⁻ showed no detectable activity, while *Δipcs*⁻/+ IPCS showed about 50% more than WT.

***Δipcs*⁻ promastigotes lack IPC.** Mass spectrometry was used to evaluate lipids present in whole cell extracts of WT, *Δipcs*⁻ and *Δipcs*⁻/+*IPCS* promastigotes (Fig. 3A-C). Two peaks corresponding to IPC were present in WT (*m/z* 778.8 and 806.8; d16:1/18:0- and d18:1/18:0 –IPC, respectively), as seen previously (Zhang, Showalter et al. 2003, Zhang, Hsu et al. 2005, Hsu, Turk et al. 2007), but were undetectable in *Δipcs*⁻ promastigotes,

[1] Data not shown.

consistent with the genetic findings. IPC levels were restored in the *Δipcs⁻/+IPCS* promastigotes, albeit only partially to about 50% WT levels (Fig. 3C).

Together with the results from enzymatic assays, these data established that *Leishmania* IPCS is the sole source of IPCS enzymatic activity or IPC.

As predicted, IPC precursor ceramide (*m/z* 536.6) levels were elevated in the *Δipcs⁻* promastigotes (Fig. 3B) relative to WT cells. However, curiously this ceramide peak did not decrease noticeably in the *Δipcs⁻/+IPCS,* despite restoration of significant IPC levels (Fig. 3C). Small variations in plasmenylethanolamine (i.e., $[M - H]^-$ ions of p18:0/18:2-PE at *m/z* 726.6 and of p18:0/18:1-PE at *m/z* 728.6) levels were also observed, but otherwise, the levels of other lipids identified by MS did not appear to change in either *Δipcs*- or *Δipcs-/*+IPCS promastigotes. These findings were not pursued further.

***Δipcs⁻* promastigotes remain viable and form metacyclics.** As promastigotes *in vitro, Δipcs⁻* grew somewhat slower than WT, with a doubling time of 9.0 ± 0.7 hours vs. 7.7 ± 0.4 hours for WT, reaching a stationary phase density of about 70% WT (Fig. 4A). Upon entry into stationary phase a small percentage of nonviable cells emerged, as judged by propidium iodide exclusion (Fig. 4B). Since *Δipcs⁻* promastigotes should retain sphingolipids capable of generating EtN (Zhang, Pompey et al. 2007), we suspected that provision of EtN would have no effect on stationary phase viability, which proved correct (Fig. S2 A,B). Restoration of IPCS expression in the *Δipcs⁻/+IPCS* line returned growth and viability to WT (Fig. 4A,B).

Upon entry into stationary phase *Leishmania* promastigotes differentiate to an infective metacyclic form that can be purified by lectin or density-gradient methods (Spath and Beverley 2001). *Δipcs⁻* showed a small reduction in metacyclics relative to

WT or the *Δipcs⁻/+IPCS* control (7.5 ± 5.3% in *Δipcs⁻* vs. 12.5 ± 8.5% in WT, or 10.7 ± 4.6%, *Δipcs⁻/+IPCS*, Fig. S2C).

***Δipcs⁻* promastigotes are hyper-susceptible to exogeneous sphingoid bases.** Accumulation of ceramide, sphingoid bases, or their phosphorylated forms is toxic to most eukaryotic cells (Hannun and Obeid 2002). This suggested that in the absence of further metabolism by IPCS, addition of exogenous sphingoid base would generate excess toxic ceramide or sphingoid bases in *Δipcs⁻*. Accordingly, daily addition of 2μM 3-keto-dihydrosphingosine, dihydrosphingosine, or C17 phytosphingosine resulted in death of *Δipcs⁻* parasites (KDS shown in Fig. 4C; others not shown[1]), which was rescued in *Δipcs⁻/+IPCS*. For cultures receiving C17 phytosphingosine, mass spectrometry confirmed synthesis of phytoceramide (Fig. S4).

***Leishmania Δipcs⁻* promastigotes are susceptible to pH but not temperature stress.** *IPCS* null *Cryptococcus neoformans* is susceptible to pH but not temperature stress (Luberto, Toffaletti et al. 2001), and we obtained similar results for *L. major Δipcs⁻* promastigotes. At pH 4.0 all cells died, while at pH 5.0, *Δipcs⁻* grew much slower (Fig. 4D), abut at pH 5.5 and above minimal differences were seen (Supplemental Table S2). Temperature stress was tested at 30º and 33º C with minimal effect on relative *Δipcs⁻* growth (Figure S3D); at 37ºC, all cells died.

Δipcs⁻ defects are not reversed by Diacylglycerol. The IPCS product DAG also functions as a messenger in multiple signaling pathways mediated by Protein Kinase C (PKC). *Leishmania* lack a known PKC although it has been suggested that other kinases may fulfill similar roles (Subramanya and Mensa-Wilmot 2010). We tested the ability of exogenous DAG to rescue the growth or viability reductions seen in *Δipcs⁻* promastigotes

by adding DAG daily to cultures. However, with two separate supplementations (0.2 and 2 μM) no improvement was observed (Figs. S2E,F), suggesting that DAG deficiency did not contribute to *Δipcs*$^-$ phenotypes.

***Δipcs*$^-$ promastigotes are rounded but lipid bodies and acidocalcisomes are unchanged.** In Δ*spt2*$^-$ promastigotes sphingolipid deficiency causes changes in cell rounding, acidocalcisomes, and lipid bodies (Zhang, Hsu et al. 2005, Zhang, Pompey et al. 2007). A modest effect on cell rounding (as defined in Zhang, Pompey et al. 2007) was observed in *Δipcs*$^-$ (22% vs. 6% for WT or 11% for *Δipcs*$^{-/}$*+IPCS*). WT and *Δipcs*$^-$ appeared similar by DAPI staining of acidocalcisomes/polyphosphates or lipids (Nile Red O staining), and *Δipcs*$^-$ acidocalcisomes appeared structurally intact as evidenced by staining with VP1 antibody (Lemercier, Dutoya et al. 2002)

***Δipcs*$^-$ remain fully virulent in mouse infections**. To test the key question of whether *IPCS* is essential for virulence, we infected Balb/c mice with 1 x 10^5 metacyclic promastigotes. Unexpectedly the *Δipcs*$^-$ infections progressed significantly faster than those of WT or *Δipcs*$^-$*/+IPC,* which were similar (a representative experiment is shown in Fig. 5 and combined data from four experiments is shown in Fig. S4A). Limiting dilution assays at key time points showed that regardless of genotype, lesions of similar sizes had similar parasite numbers (Fig. S4B). These data establish that if anything *Δipcs*$^-$ was unexpectedly somewhat hypervirulent.

***ipcs*- amastigotes lack IPC.** To eliminate the possibility that amastigotes elaborated an alternative IPCS activity, parasites were harvested and purified from similarly sized lesions in Balb/c mice, and lipids were extracted for analysis by electrospray ionization mass spectrometry (ESI/MS) in the negative ion mode. High amounts of background

signal limited interpretations of full spectra, but product ion scan of the 241 m/z $[M – H]^-$ ion specific for detection of PtI and IPC lipids (Hsu, Turk et al. 2007) (Hsu and Turk 2000) failed to detect IPC in *Δipcs*$^-$ amastigotes (Fig. 6D, E), in four separate preparations. Otherwise, the abundance of other lipid species did not appear to change consistently, with the possible exception of 18:0/20:4-PtI (*m/z* 885) which was elevated in 2/4 *Δipcs*$^-$ amastigote preparations the reasons for this are unclear. IPC production was restored in *Δipcs*$^-$*/+IPCS* amastigotes[1]. Thus, *Δipcs*$^-$ *L. major* amastigotes readily survive and induce pathology without IPC.

Wild type amastigotes contain abundant amounts of host derived sphingomyelin. Functional genetic studies suggested that *Leishmania* amastigotes may salvage and degrade host sphingomyelin (Zhang, Wilson et al. 2009). We examined this more directly by MS in the amastigote stage, in both WT and *Δipcs*$^-$ parasites. Employing ESI/MS in the positive ion mode, we observed highly abundant amounts of SM in both WT and *Δipcs*$^-$ purified amastigotes (Fig. 6 A,B). Since purified amastigotes typically are contaminated by host material, we extracted lipids from total infected footpad lesions where the mouse contaminants dominate for comparison (Fig. 6C).

In purified WT amastigotes, SM (d18:1/16:0 SM; *m/z* 725) levels were reduced 1.3-fold, while the other SM level including d18:1/22:0 SM (*m/z* 809), d18:1/24:2 (m/z 833), and d18:1/24:1 (m/z 835) were only slightly altered or unchanged relative to infected tissues (Fig.6A,B,C; representative spectra from 2 expts and 3 replicas showed similar findings). That this largely reflects parasite-derived lipids is supported by the finding that known mouse-specific lipids were greatly reduced in the purified amastigote preparations, with PtC species reduced about 16 fold (range 9-26) and plasmanyl choline

reduced about 4 fold (range 2.6 – 4.8). These data suggest that the most of the SM seen in purified WT or *Δipcs*⁻ amastigotes arises from the parasite itself.

As discussed above, ESI/MS revealed the presence of abundant IPC species in purified WT but not *Δipcs*⁻ amastigotes (Fig. 6D, E). In further support of the minimal parasite contributions to the infected tissue sample lipids, parasite-specific IPC species were barely detectable (Fig. 6F). Interestingly, a number of PtI species with similar m/z were seen were elevated in WT vs. *Δipcs*⁻ in purified amastigotes, the significance of which is unknown (data not shown). .

Salvaged SM and not IPC is the predominant SL in amastigotes. An important question was the relative amounts of IPC and SM in amastigotes. In previous studies we added non-biological standards expected to have similar MS ionization behavior, titrating the amounts in pilot studies until a similar peak height was obtained with the biological species of interest (Zhang, Hsu et al. 2005). The results from a representative amastigote preparation spiked with 10 nmol N-Lauryl SM and 2 nmol of dipalmitoyol phosphoinositol, followed by positive or negative ion MS are shown in Figure 7. Given that the SM/standard and IPC/standard peaks were of similar intensity, and that most SM was contributed by the parasite (Fig. 6), we concluded from the standard ratios that the ratio of parasite IPC to SM is about 1:5 in amastigotes (similar results were seen in 2 independent experiments). The sensitivity of this 'spike-in' our assay did not allow us to estimate differences in the abundance of SM between WT and *Δipcs*⁻ amastigotes; however, no obvious differences were observed (Fig. 6). Thus and perhaps unexpectedly, SM is the dominant sphingolipid in amastigotes despite their capacity for IPC synthesis.

Wild type amastigotes contain IPC with mammalian-like ceramide anchor. Previous findings suggested that SL degradation by ISCL is required for pathology (Fig. 3) (Zhang, Showalter et al. 2003, Zhang, Wilson et al. 2009), which lead us to consider whether the amastigote IPC anchor might arise from salvage of mammalian SLs, most likely SM (Fig. 6). The ceramide anchor of mammalian sphingomyelin has a structure of d18:1/16:0, while promastigote IPC has a subtly different structure of d16:1/18:0 (Hsu, Turk et al. 2007, Dennis, Deems et al. 2010). The MS^2 product ion spectra of the IPC *m/z* 778 ion from both parasite stages (Fig. 8 A) exhibited a peak at *m/z* 598, from the loss of inositol (Hsu, Turk et al. 2007). In promastigotes, MS3 fragmentation this generates an 18:0 fatty acid carboxylate at *m/z* 283, together with ions of m/z 332 and 314 arising from loss of 18:0-FA as acid and ketene, respectively (Fig. 8C). In contrast, in amastigotes, MS^3 fragmentation of this species produces a 16:0 fatty acid carboxylate at *m/z* 255, along with ions of m/z 360 and 342 arising from loss of 16:0-FA as acid and ketene, respectively (Fig. 8B). \

Therefore, unlike promastigote IPC whose anchor is d16:1/18:0, that of amastigote IPC is d18:1/16:0 IPC, the same as that of mammalian SM. This suggests the amastigote IPC anchor arises primarily through salvage rather than by *de novo* synthesis, accounting for its retention in *Δspt2*$^-$ amastigotes lacking *de novo* SL synthesis (Zhang, Showalter et al. 2003).

Discussion

Here we describe the virulence and phenotypic characteristics of *IPCS*-null *L. major* as well as advances in our understanding of host sphingolipid salvage by amastigotes. In contrast to other eukaryotic microbes, *IPCS*-null (*Δipcs*$^-$) parasites could

be readily obtained (Fig. 1), which as promastigotes appeared nearly normal, with small differences in cell shape, growth and viability (Fig. 4A,B). *Δipcs*⁻ promastigotes lacked IPCS enzymatic activity (Figs. 2, S1), and both promastigotes and amastigotes lacked IPC (Figs. 3, 6), ruling out alternatives sources of IPC synthesis across the infectious cycle. We also confirmed that endogenously synthesized IPCS was insensitive to auerobasidin A, as seen with recombinant enzyme (Fig. 2) (Sevova, Goren et al. 2010). In all studies, ectopic re-expression of IPCS restored IPC synthesis and indeed any other phenotype shown (Figs. 3-5). IPCS activity consumes ceramide and PtI to yield IPC and DAG, however the health of *Δipcs*⁻ suggests that perturbations of these substrates in this context have little deleterious effect during the infectious cycle. Provision of high levels of exogenous DAG had little effect on *Δipcs*⁻ but feeding sphingoid bases proved toxic to *Δipcs*⁻, presumably due to accumulation of sphingoid bases and ceramide as seen in *Leishmania* and fungi (Hannun and Obeid 2002, Zhang, Hsu et al. 2013). *Δipcs*⁻ was strongly inhibited relative to WT when grown at pH 5 (Fig. 4D), however this effect was largely ameliorated at pH 5.5 or above (Supplemental Table 2). This is consistent with the survival of *Δipcs*⁻ in animal infections (Fig. 5), as the *Leishmania major* parasitophorous vacuole has a pH of 5.4 (Spath, Schlesinger et al. 2009) which would only weakly impact *Δipcs*⁻. In these properties, *Leishmania* differs significantly from *Cryptococcus neoformans*, where IPCS is essential and IPCS-deficient organisms are hyper-susceptible to pH stress through an absence of DAG signaling (Luberto, Toffaletti et al. 2001).

In distinct contrast to other eukaryotic microbes, *Δipcs*⁻ *L. major* showed no defects in virulence as revealed by their ability to survive and induce progressive

pathology when inoculated into susceptible mice (Figs. 5, S4A). In fact, lesion pathology was somewhat enhanced in the *Δipcs*⁻, as was the parasite burden (Fig. 5, S4B). Several studies have reported interactions between *Leishmania* and host ceramide impacting macrophage survival of the related species *L. donovani* (Ghosh, Bhattacharyya et al. 2001, Ghosh, Bhattacharyya et al. 2002) and the modest hypervirulence seen with *L. major Δipcs*⁻ may arise from similar effects.

Leishmania promastigotes can survive perfectly well without any cellular SLs (Zhang, Showalter et al. 2003, Denny, Goulding et al. 2004), raising the possibility that the amastigote stage may likewise lack a requirement for SLs. However, *Leishmania* sp. are known to take up and salvage a variety of host lipids including SM (McConville and Naderer 2011, Zhang 2021). This raised the possibility that any potential amastigote-stage SL requirement could be satisfied by swapping endogenous IPC by salvage with host SM. Indeed, MS analysis of purified amastigotes showed high levels of host SM, in both WT and *Δipcs*⁻, and semi-quantitative analysis of WT showing that host SM was about 5-fold more abundant than parasite IPC. Thus even in WT parasites, uptake of host SM leads to predominance over endogenous IPC synthesis. This suggests the possibility that loss of IPC in *Δipcs*⁻ might result in only a slight reduction in total SLs which could be overcome by a small increase in salvage. Currently the mechanism by which SM is acquired by the parasite is unknown. Since no *Leishmania* mutants have been identified where amastigotes completely lack SLs, the question of the absolute amastigote requirement for SLs remains enigmatic. Moreover, *Leishmania*, salvage abundant amounts of SM and the exact role for this rather than reliance on IPC remains unclear. Possible explanations include molecular mimicry to hide the parasite from the innate

immune system or reduction of the pool of host lipids and signaling pathways. The vital roles of SLs in *L. major* pathology suggests further studies may uncover unique pathways amenable to therapeutic intervention.

Interestingly, the structure of the ceramide anchor of WT amastigote IPC corresponds not to that of the WT promastigote (d16:1/18:0) but instead mirrors that of host SM (d18:1/16:0; Fig 8). Previously we showed that the *SPT2* subunit of the key *de novo* sphingoid base synthetic enzyme, serine palmitoyl transferase, is not synthesized by the amastigote stage (Zhang, Showalter et al. 2003, Denny, Goulding et al. 2004). This suggests that unlike promastigotes which synthesize ceramide as well, amastigotes instead acquire the IPC anchor precursor ceramide from host SM, presumably through the action of the parasite ISCL, the ortholog of the fungal enzyme inositol phosphosphingolipid phospholipase C which but which instead shows 20-fold stronger activity with SM (Zhang, Wilson et al. 2009).

A significant and unambiguous finding was that neither IPC nor IPCS are essential at *any* point in the parasite infectious cycle, unlike pathogenic fungi where IPCS is an essential enzyme with considerable potential as a drug target. In this respect, our data do not provide much optimism for IPCS as a drug target in the *Leishmania* parasite. While some previous studies have suggested the activity of yeast IPCS inhibitor auerobasidin A potentially provided chemical validation of *Leishmania* IPCS, it has a high IC_{50} and is inactive against recombinant IPCS from trypanosomes and *Leishmania* (Denny, Shams-Eldin et al. 2006, Sevova, Goren et al. 2010). Whether other candidate inhibitors showing activity against cultured parasites (Figueiredo, Dias et al. 2005, Mina, Mosely et al. 2010, Sevova, Goren et al. 2010, Mina, Mosely et al. 2011) act ‘on target’

against *Leishmania* IPCS remains to be seen, although the health of the *Δipcs*⁻ mutant suggest this may be unlikely. *In vitro*, IPCS inhibitors may act synergistically with other compounds[1], although whether this extends to the *in vivo* situation with abundant SL salvage remains to be seen.

Our studies thus provide a new perspective on *Leishmania* SL pathways, emphasizing the role of SM salvage from the host cell over *de novo* synthesis by the amastigote stage, additionally raising many interesting questions that will require further study. Instead, our findings with IPCS or previous studies with ISCL suggest that agents inhibit SL salvage or catabolism in *Leishmania* may have more promise as chemotherapeutic agents.

Experimental Procedures

Molecular constructs. Molecular constructs containing 610 bp of 5' flanking (Primers SMB 2590, 2591; Table S1 contain the sequences of all oligonucleotides used) and 665 bp of 3' flanking (SMB 2592, 2593) sequence flanking the *IPCS* ORF were joined by fusion PCR to the ORF for the selectable markers NEO (SMB2586, 2587) or SAT (SMB 2588, 2589). These constructs (pGEM T Easy-IPCS::ΔNEO, B5810, or pGEM T Easy-IPCS::ΔSAT, B6075) were linearized by digestion with EcoRI to expose the homologous ends prior to electroporation. To restore IPCS expression, the IPCS coding region (Lm35.4990) was amplified by PCR using the primers SMB 3259 and 3260 and inserted into the pXG expression vector (Ha, Schwarz et al. 1996, Goyard and Beverley 2000) yielding pXG-BSD-IPCS (B6235). All constructs were confirmed by sequencing.

***Leishmania* culture and transfection.** *Leishmania major* (LV39 clone 5, Rho/SU/59/P) was grown in M199 media supplemented with 10% fetal bovine serum, 12 mM $NaHCO_3$, 0.1 mM adenine, 7.6 mM hemin, 2 μg/ml biopterin, 20 μM Folic Acid, 1x RPMI Vitamin Mix, 2mM glutamine, 25 mM HEPES pH 6.8, 50 U/ml penicillin, and 50 μg/ml streptomycin (Goyard, Segawa et al. 2003). Cell density was measured using a coulter counter (Becton Dickinson) and viability was determined by flow cytometry (Becton Dickinson) after staining with 5μg/ml propidium iodide. In some experiments supplements were added as indicated, or the pH was altered as shown in table S1 and MES or citrate buffers. Metacyclic cells were prepared by density purification or PNA-purification as described (Spath and Beverley 2001).

Transfections were performed by electroporation as previously described (Kapler, Coburn et al. 1990). To replace the first IPCS allele, transfection with the *IPCS:: ΔNEO* targeting fragment was performed; due to some media/serum concerns at the time these studies were undertaken, we had difficulty recovering transfectant colonies by our usual plating procedures. Thus, after electroporation and a 24 hr recovery period in 3 separate pools, clonal lines were obtained by limiting dilution in M199 medium containing 10 μg/ml neomycin and 500 μM EtN. The authenticity of several putative heterozygous transfectants (*IPCS / IPCS:: ΔNEO*) was confirmed by PCR. Correct integration was confirmed by using primers outside the flanking region and inside the drug marker (SMB2598/2600 5'Flank and SMB2608/2827 3'Flank). Several independent clonal lines were inoculated into susceptible BALB/c mice (10^7 parasites/footpad) and recovered after 1 month; such lines are referred to as M1 passage. Two such lines (WA and WB) were then transfected with the *IPCS:: ΔSAT* targeting fragment, resistant cells obtained

following growth in 8 μg/ml neomycin and 100 μg/ml nourseothricin, and clonal lines obtained by limiting dilution. The authenticity of potential homozygous Δ*ipcs*⁻ null mutants (formally *IPCS:: ΔNEO/IPCS:: ΔSAT*) was confirmed by PCR as described above using primers SMB 2598/2601 (5' flank) and SMB 2609/2827 (3' Flank). Several lines were inoculated into BALB/c mice as before. IPCS expression was restored in several Δ*ipcs*⁻ M1 transfectants (WAB, WAD, and WAE) by transfection with pXG-BSD-IPCS (B6235) to generate *ipcs::* Δ*NEO/ipcs::* Δ*SAT/+pXG-IPCS*, referred to as Δ*ipcs*⁻/+*IPCS*. As all transfectant and add-back lines showed similar behavior in preliminary tests, detailed studies are presented only for clone WAD (Δ*ipcs*⁻) or WADB (Δ*ipcs*⁻/+*IPCS*) unless otherwise stated.

Microsomal Preparation and Enzyme Assays. Microsomes were prepared by washing 4 x 10^8 promastigotes in PBS and homogenized by sonication in buffer (50mM MES, 50mM BIS-TRIS pH 6.25, 10mM EDTA, 100mM NaCl, 250 mM Sucrose, 300 nM aprotinin, 1 mM benzamidine, 1μg/ml chymostatin and pepstatin, 10 μM E64 and leupeptin, 10 mM NaF). Debris was removed by centrifugation at 1,000 x g for 10 min and the supernatant was then centrifuged at 100,000 x g for 90 minutes. The pellet was resuspended in minimal amounts of buffer (5 mM MES, 5 mM BIS_TRIS pH 6.25, 1 mM EDTA, 100 mM NaCl, 15 % glycerol, 300nM aprotinin, 1mM benzamidine, 1μg/ml chymostatin and pepstatin, 10 μM E64 and leupeptin, 1 mM NaF) with sonication then flash frozen. Protein content was determined by BCA assay using BSA standards.

Enzyme assays were performed in 100 μl IPCS assay buffer (100mM MES, 100mM BIS-TRIS pH 6.25, 5mM EDTA, 100mM NaCl, 300nM aprotinin, 1mM benzamidine, 1μg/ml chymostatin and pepstatin, 10 μM E64 and leupeptin, 1 mM NaF)

Lipid substrates were dried by speedvac prior to resuspension is assay buffer, using 625 picomoles of L-α-phosphatidylinositol from soy and 250 picomoles of NBD-C_6-Ceramide unless otherwise indicated. 25 μg of microsomal protein was added to the reactions which were incubated at 28°C for 60 minutes and terminated with 500 μl of 50 mM HCl in methanol. Lipids were extracted with 1.5 ml of chloroform and 463 μl of 1M NaCl. Samples were vortexed and centrifuged at 1,500 x g for 5 min. The upper phase was re-extracted with 750 μl of chloroform:methanol (43:7) and the combined lower phases were dried by nitrogen stream. Samples were resuspended in 50 μl of chloroform:methanol (2:1) and 5 μl were loaded on predeveloped Baker Si-250-PA 60 A silica gel TLC plates and developed using chloroform:methanol:water:ammonium hydroxide (28%)/65:30:3:2/v:v:v:v. Images were developed using Fuji FLA-5000 phosphoimager.

Lipid Extraction. Promastigotes were collected from 100 ml cultures and lesion amastigotes were harvested as described (Akopyants, Matlib et al. 2004). Sphingolipids from log phase promastigotes or amastigotes were extracted using a modified Folch extraction. First, 2 x 10^8 cells were resuspended in 1.5 ml 25 mM Sodium Fluoride with 2 ml Methanol and sonicated. Next, 4 ml of chloroform was added; samples were vortexed and centrifuged at 1,800 x g for 15 minutes. The upper phase was re-extracted with 2.5 ml of chloroform:methanol (43:7), vortexed, and centrifuged. Combined lower phases were back extracted with 2 ml of 50 mM sodium fluoride and 2 ml of Methanol, vortexed, and centrifuged. The lower phase was dried by nitrogen stream and extracted again with chloroform:methanol:50mM sodium fluoride (4:2:1), vortexed, and

centrifuged. The lower phase was again dried by nitrogen stream and resuspended in 1 ml of chloroform:methanol (1:1) for analysis by mass spectrometry.

Mass Spectrometry. ESI/MS analyses were performed on a Thermo Scientific (San Jose, CA) triple stage quadrupole (TSQ) Vantage EMR mass spectrometer with Xcalibur operating system. Lipid extracts (10uL each injection) were loop injection to the HESI-II probe in a Thermo Scientific™ Ion Max ion source by a built-in syringe pump which delivered a constant flow of methanol at 20uL/min. The mass spectrometer was tuned to unit-mass resolution, and the heated capillary temperature was set to 280°C. The electrospray needle was set at 4.0 kV and 3.5 kV for positive-ion and negative-ion modes operation, respectively, and the skimmer was at ground potential. The mass resolution of both Q1 and Q3 was set at 0.6 Da at half peak height to obtain the product-ion scan, precursor ion scan and neutral loss scan (NLS) mass spectra, using a collision energy of 30-40 eV with target gas of Ar (1.3 mtorr) in the rf-only second quadrupole (Q2). The mass spectra were accumulated in the profile mode.

Mouse Virulence. Mouse experiments were done in compliance with policies approved by the Animal Review Board at Washington University. Briefly, Balb/c mice were infected with 10^5 metacyclics purified by gradient centrifugation (Spath and Beverley 2001), and footpad lesion swelling measured weekly, and at key points parasites were enumerated by limiting dilution assays (Titus, Marchand et al. 1985).

Supporting information.

This article contains supporting information available on-kine.

Acknowledgments.

We thank the members of our laboratory and Kai Zhang (Texas Tech University, Lubbock) for helpful discussions. This manuscript was submitted posthumously on behalf of John Turk.

Author contributions.

FMK, PK, FH and SMB, conceptualization; FMK, PK, SH and FH, investigations, FMK, FH and SMB, writing.

Funding.

Supported by NIH Grant AI31078 to SMB and the Division of Infectious Diseases, Washington University (FMK). The Mass Spectrometry Resource of Washington University is supported by NIH grants P30DK020579, P30DK056341, and P41GM103422.

Conflict of interest.

The authors declare that they have no conflicts of interest with the contents of this article.

Abbreviations.

WT, wild-type *Leishmania major*; IPC, inositolphorphorylceramide; IPCS, inositolphosphorylceramide synthase; SL, sphingolipid; SLS, sphingolipid synthase; PtC, phosphatidyl choline; PtI, phosphatidyl insotiol; PI-PLC, phosphatidyl inositol phospholipase C; NBD-Cer, (6-((N-(7-Nitrobenz-2-Oxa-1,3-Diazol-4-yl)amino)hexanoyl)Sphingosine); MS,mass spectrometry; ISCL, inositol phosphorylceramide phosolipase C-like; ESI/MS, electrospray ionization mass spectrometry.

References

Akopyants, N. S., R. S. Matlib, E. N. Bukanova, M. R. Smeds, B. H. Brownstein, G. D. Stormo and S. M. Beverley (2004). "Expression profiling using random genomic DNA microarrays identifies differentially expressed genes associated with three major developmental stages of the protozoan parasite Leishmania major." Mol Biochem Parasitol **136**(1): 71-86.

Ali, H. Z., C. R. Harding and P. W. Denny (2011). "Endocytosis and Sphingolipid Scavenging in Leishmania mexicana Amastigotes." Biochem Res Int **2012**: 691363.

Alvar, J., I. D. Velez, C. Bern, M. Herrero, P. Desjeux, J. Cano, J. Jannin and M. den Boer (2012). "Leishmaniasis worldwide and global estimates of its incidence." PLoS One **7**(5): e35671.

Banuls, A. L., P. Bastien, C. Pomares, J. Arevalo, R. Fisa and M. Hide (2011). "Clinical pleiomorphism in human leishmaniases, with special mention of asymptomatic infection." Clin Microbiol Infect **17**(10): 1451-1461.

Cohen, J. A., F. Barkhof, G. Comi, H. P. Hartung, B. O. Khatri, X. Montalban, J. Pelletier, R. Capra, P. Gallo, G. Izquierdo, K. Tiel-Wilck, A. de Vera, J. Jin, T. Stites, S. Wu, S. Aradhye and L. Kappos (2010). "Oral fingolimod or intramuscular interferon for relapsing multiple sclerosis." N Engl J Med **362**(5): 402-415.

Croft, S. L., S. Sundar and A. H. Fairlamb (2006). "Drug resistance in leishmaniasis." Clin Microbiol Rev **19**(1): 111-126.

Cruz, A., C. M. Coburn and S. M. Beverley (1991). "Double targeted gene replacement for creating null mutants." Proc Natl Acad Sci U S A **88**(16): 7170-7174.

den Boer, M., D. Argaw, J. Jannin and J. Alvar (2011). "Leishmaniasis impact and treatment access." Clin Microbiol Infect **17**(10): 1471-1477.

Dennis, E. A., R. A. Deems, R. Harkewicz, O. Quehenberger, H. A. Brown, S. B. Milne, D. S. Myers, C. K. Glass, G. Hardiman, D. Reichart, A. H. Merrill, Jr., M. C. Sullards, E. Wang, R. C. Murphy, C. R. Raetz, T. A. Garrett, Z. Guan, A. C. Ryan, D. W. Russell, J. G. McDonald, B. M. Thompson, W. A. Shaw, M. Sud, Y. Zhao, S. Gupta, M. R. Maurya, E. Fahy and S. Subramaniam (2010). "A mouse macrophage lipidome." J Biol Chem **285**(51): 39976-39985.

Denny, P. W., D. Goulding, M. A. Ferguson and D. F. Smith (2004). "Sphingolipid-free Leishmania are defective in membrane trafficking, differentiation and infectivity." Mol Microbiol **52**(2): 313-327.

Denny, P. W., H. Shams-Eldin, H. P. Price, D. F. Smith and R. T. Schwarz (2006). "The protozoan inositol phosphorylceramide synthase: a novel drug target that defines a new class of sphingolipid synthase." J Biol Chem **281**(38): 28200-28209.

Figueiredo, J. M., W. B. Dias, L. Mendonca-Previato, J. O. Previato and N. Heise (2005). "Characterization of the inositol phosphorylceramide synthase activity from Trypanosoma cruzi." Biochem J **387**(Pt 2): 519-529.

Ghosh, S., S. Bhattacharyya, S. Das, S. Raha, N. Maulik, D. K. Das, S. Roy and S. Majumdar (2001). "Generation of ceramide in murine macrophages infected with Leishmania donovani alters macrophage signaling events and aids intracellular parasitic survival." Mol Cell Biochem **223**(1-2): 47-60.

Ghosh, S., S. Bhattacharyya, M. Sirkar, G. S. Sa, T. Das, D. Majumdar, S. Roy and S. Majumdar (2002). "*Leishmania donovani* suppresses activated protein 1 and NF-kappaB activation in host macrophages via ceramide generation: involvement of extracellular signal-regulated kinase." Infect Immun **70**(12): 6828-6838.

Goyard, S. and S. M. Beverley (2000). "Blasticidin resistance: a new independent marker for stable transfection of Leishmania." Mol Biochem Parasitol **108**(2): 249-252.

Goyard, S., H. Segawa, J. Gordon, M. Showalter, R. Duncan, S. J. Turco and S. M. Beverley (2003). "An in vitro system for developmental and genetic studies of Leishmania donovani phosphoglycans." Mol Biochem Parasitol **130**(1): 31-42.

Guan, X. L. and P. Maser (2017). "Comparative sphingolipidomics of disease-causing trypanosomatids reveal unique lifecycle- and taxonomy-specific lipid chemistries." Sci Rep **7**(1): 13617.

Ha, D. S., J. K. Schwarz, S. J. Turco and S. M. Beverley (1996). "Use of the green fluorescent protein as a marker in transfected Leishmania." Mol Biochem Parasitol **77**(1): 57-64.

Hannun, Y. A. and L. M. Obeid (2002). "The Ceramide-centric universe of lipid-mediated cell regulation: stress encounters of the lipid kind." J Biol Chem **277**(29): 25847-25850.

Hannun, Y. A. and L. M. Obeid (2018). "Sphingolipids and their metabolism in physiology and disease." Nat Rev Mol Cell Biol **19**(3): 175-191.

Harrison, P. J., T. M. Dunn and D. J. Campopiano (2018). "Sphingolipid biosynthesis in man and microbes." Nat Prod Rep **35**(9): 921-954.

Heidler, S. A. and J. A. Radding (2000). "Inositol phosphoryl transferases from human pathogenic fungi." Biochim Biophys Acta **1500**(1): 147-152.

Herwaldt, B. L. (1999). "Leishmaniasis." Lancet **354**(9185): 1191-1199.

Hsu, F. F. and J. Turk (2000). "Characterization of phosphatidylinositol, phosphatidylinositol-4-phosphate, and phosphatidylinositol-4,5-bisphosphate by electrospray ionization tandem mass spectrometry: a mechanistic study." J Am Soc Mass Spectrom **11**(11): 986-999.

Hsu, F. F., J. Turk, K. Zhang and S. M. Beverley (2007). "Characterization of inositol phosphorylceramides from Leishmania major by tandem mass spectrometry with electrospray ionization." J Am Soc Mass Spectrom **18**(9): 1591-1604.

Kaneshiro, E. S., K. Jayasimhulu and R. L. Lester (1986). "Characterization of inositol lipids from Leishmania donovani promastigotes: identification of an inositol sphingophospholipid." J Lipid Res **27**(12): 1294-1303.

Kapler, G. M., C. M. Coburn and S. M. Beverley (1990). "Stable transfection of the human parasite Leishmania major delineates a 30-kilobase region sufficient for extrachromosomal replication and expression." Mol Cell Biol **10**(3): 1084-1094.

Koeller, C. M. and N. Heise (2011). "The Sphingolipid Biosynthetic Pathway Is a Potential Target for Chemotherapy against Chagas Disease." Enzyme Res **2011**: 648159.

Lemercier, G., S. Dutoya, S. Luo, F. A. Ruiz, C. O. Rodrigues, T. Baltz, R. Docampo and N. Bakalara (2002). "A vacuolar-type H+-pyrophosphatase governs maintenance of functional acidocalcisomes and growth of the insect and mammalian forms of Trypanosoma brucei." J Biol Chem **277**(40): 37369-37376.

Luberto, C., D. L. Toffaletti, E. A. Wills, S. C. Tucker, A. Casadevall, J. R. Perfect, Y. A. Hannun and M. Del Poeta (2001). "Roles for inositol-phosphoryl ceramide synthase 1 (IPC1) in pathogenesis of C. neoformans." Genes Dev **15**(2): 201-212.

Mannan, S. B., H. Elhadad, T. T. H. Loc, M. Sadik, M. Y. F. Mohamed, N. H. Nam, N. D. Thuong, B. L. Hoang-Trong, N. T. M. Duc, A. N. Hoang, K. M. Elhusseiny, L. H. N. Minh, T. T. H. Quynh, T. L. B. Nghia, Y. Mai Nhu, T. M. Tieu, K. Hirayama, N. T. Huy and S. Hamano (2021). "Prevalence and associated factors of asymptomatic leishmaniasis: a systematic review and meta-analysis." Parasitol Int **81**: 102229.

McConville, M. J. and T. Naderer (2011). "Metabolic pathways required for the intracellular survival of Leishmania." Annu Rev Microbiol **65**: 543-561.

Megyeri, M., H. Riezman, M. Schuldiner and A. H. Futerman (2016). "Making Sense of the Yeast Sphingolipid Pathway." J Mol Biol **428**(24 Pt A): 4765-4775.

Mina, J. G., J. A. Mosely, H. Z. Ali, P. W. Denny and P. G. Steel (2011). "Exploring Leishmania major Inositol Phosphorylceramide Synthase (LmjIPCS): Insights into the ceramide binding domain." Org Biomol Chem.

Mina, J. G., J. A. Mosely, H. Z. Ali, H. Shams-Eldin, R. T. Schwarz, P. G. Steel and P. W. Denny (2010). "A plate-based assay system for analyses and screening of the Leishmania major inositol phosphorylceramide synthase." Int J Biochem Cell Biol **42**(9): 1553-1561.

Mina, J. G. M. and P. W. Denny (2018). "Everybody needs sphingolipids, right! Mining for new drug targets in protozoan sphingolipid biosynthesis." Parasitology **145**(2): 134-147.

Norcliffe, J. L., J. G. Mina, E. Alvarez, J. Cantizani, F. de Dios-Anton, G. Colmenarejo, S. G. Valle, M. Marco, J. M. Fiandor, J. J. Martin, P. G. Steel and P. W. Denny (2018). "Identifying inhibitors of the Leishmania inositol phosphorylceramide synthase with antiprotozoal activity using a yeast-based assay and ultra-high throughput screening platform." Sci Rep **8**(1): 3938.

Oskouian, B. and J. D. Saba (2010). "Cancer treatment strategies targeting sphingolipid metabolism." Adv Exp Med Biol **688**: 185-205.

Pigott, D. M., S. Bhatt, N. Golding, K. A. Duda, K. E. Battle, O. J. Brady, J. P. Messina, Y. Balard, P. Bastien, F. Pratlong, J. S. Brownstein, C. C. Freifeld, S. R. Mekaru, P. W. Gething, D. B. George, M. F. Myers, R. Reithinger and S. I. Hay (2014). "Global distribution maps of the leishmaniases." Elife **3**: e28051.

Sangshetti, J. N., F. A. K. Khan, A. K. Kulkarni, R. Arote and R. H. Patil (2015). " DOI: 10.1039/C5RA02669E (Review Article) RSC Adv., 2015, 5, 32376-32415

Antileishmanial drug discovery: comprehensive review of the last 10 years

" Royal Society of Chemistry **5**: 32376-32415.

Sevova, E. S., M. A. Goren, K. J. Schwartz, F. F. Hsu, J. Turk, B. G. Fox and J. D. Bangs (2010). "Cell-free synthesis and functional characterization of sphingolipid synthases from parasitic trypanosomatid protozoa." J Biol Chem **285**(27): 20580-20587.

Singh, O. P., E. Hasker, D. Sacks, M. Boelaert and S. Sundar (2014). "Asymptomatic Leishmania infection: a new challenge for Leishmania control." Clin Infect Dis **58**(10): 1424-1429.

Spath, G. F. and S. M. Beverley (2001). "A lipophosphoglycan-independent method for isolation of infective Leishmania metacyclic promastigotes by density gradient centrifugation." Exp Parasitol **99**(2): 97-103.

Spath, G. F., P. Schlesinger, R. Schreiber and S. M. Beverley (2009). "A novel role for Stat1 in phagosome acidification and natural host resistance to intracellular infection by *Leishmania major*." PLoS Pathog **5**(4): e1000381.

Subramanya, S. and K. Mensa-Wilmot (2010). "Diacylglycerol-stimulated endocytosis of transferrin in trypanosomatids is dependent on tyrosine kinase activity." PLoS One **5**(1): e8538.

Sutterwala, S. S., F. F. Hsu, E. S. Sevova, K. J. Schwartz, K. Zhang, P. Key, J. Turk, S. M. Beverley and J. D. Bangs (2008). "Developmentally regulated sphingolipid synthesis in African trypanosomes." Mol Microbiol **70**(2): 281-296.

Suzuki, E., A. K. Tanaka, M. S. Toledo, S. B. Levery, A. H. Straus and H. K. Takahashi (2008). "Trypanosomatid and fungal glycolipids and sphingolipids as infectivity factors and potential targets for development of new therapeutic strategies." Biochim Biophys Acta **1780**(3): 362-369.

Titus, R. G., M. Marchand, T. Boon and J. A. Louis (1985). "A limiting dilution assay for quantifying *Leishmania major* in tissues of infected mice." Parasite Immunol. **7**: 545-555.

WHO (2010). "Control of the Leishmaniases: WHO Expert Committee on the Control of Leishmaniases." World Health Organization Technical Reports **949**: 1-186.

Winter, G., M. Fuchs, M. J. McConville, Y. D. Stierhof and P. Overath (1994). "Surface antigens of Leishmania mexicana amastigotes: characterization of glycoinositol phospholipids and a macrophage-derived glycosphingolipid." J Cell Sci **107 (Pt 9)**: 2471-2482.

Zhang, K. (2021). "Balancing de novo synthesis and salvage of lipids by Leishmania amastigotes." Curr Opin Microbiol **63**: 98-103.

Zhang, K., J. D. Bangs and S. M. Beverley (2010). "Sphingolipids in parasitic protozoa." Adv Exp Med Biol **688**: 238-248.

Zhang, K., F. F. Hsu, D. A. Scott, R. Docampo, J. Turk and S. M. Beverley (2005). "Leishmania salvage and remodelling of host sphingolipids in amastigote survival and acidocalcisome biogenesis." Mol Microbiol **55**(5): 1566-1578.

Zhang, K., J. M. Pompey, F. F. Hsu, P. Key, P. Bandhuvula, J. D. Saba, J. Turk and S. M. Beverley (2007). "Redirection of sphingolipid metabolism toward de novo synthesis of ethanolamine in Leishmania." Embo J **26**(4): 1094-1104.

Zhang, K., M. Showalter, J. Revollo, F. F. Hsu, J. Turk and S. M. Beverley (2003). "Sphingolipids are essential for differentiation but not growth in Leishmania." Embo J **22**(22): 6016-6026.

Zhang, O., F. F. Hsu, W. Xu, M. Pawlowic and K. Zhang (2013). "Sphingosine kinase A is a pleiotropic and essential enzyme for Leishmania survival and virulence." Mol Microbiol **90**(3): 489-501.

Zhang, O., M. C. Wilson, W. Xu, F. F. Hsu, J. Turk, F. M. Kuhlmann, Y. Wang, L. Soong, P. Key, S. M. Beverley and K. Zhang (2009). "Degradation of host sphingomyelin is essential for Leishmania virulence." PLoS Pathog **5**(12): e1000692.

Figure Legends

Figure 1: Generation of *Δipcs*⁻ promastigotes.
(A) Schematic of planned replacements for *IPCS* with drug markers for nourseothricin (*SAT*), G418 (*NEO*) and expression construct pXG-IPCS with blasticidin (*BSD*) resistance. Arrows represent the location of primers used for PCR; Primers 1/4 and 3/2 tests for correct *NEO* 5'and 3' replacements; primers 1/6 and 5/2 test for correct *SAT* 5' and 3' replacement; primers 7/2 tests for WT *IPCS* and 7/8 test for the pXG-born *IPCS*. Primer 1, SMB 2598; 2, SMB 22827; 3, SMB 2600; 4, SMB 2608; 5, SMB 2609; 6, SMB 2601; 7, SMB 2607; and 8, SMB 1421. (B) PCR confirmation of parasite transfectants. *IPCS*::*NEO* replacement (lanes 1,2, primers 1+4, expected size 860bp; and 3+2, expected size 1024bp); planned *IPCS::SAT* replacement (lanes 3,4, primers 1+6, expected size 849bp; and 5+2 , expected size 933bp); WT *IPCS* (lane 5, primers 7+2, expected size 882bp); and pXG-BS-IPCS (lane 6, primers 7+8, expected size 124bp).

Figure 2: Enzymatic characterization of IPCS activity and its absence in Δ*ipcs*⁻ promastigotes.
(A) NBD-IPC formation in complete reactions, or in the absence of key substrates, microsomes, inhibitors or enzymatic treatments as indicated. (B) Quantitation of NBD-IPC formation by microsomes from WT, Δ*ipcs*⁻ or Δ*ipcs*⁻/+*IPCS* parasites Primary TLC data can be found in Fig. S1.

Figure 3: Absence of IPC in Δ*ipcs*⁻ *Leishmania*. The figure shows the ESI/MS spectrum (negative ion mode) obtained with lipid preparations from logarithmic growth phase WT, Δ*ipcs*⁻, or Δ*ipcs*⁻/+*IPCS* promastigotes.

Figure 4: Phenotypic characterization of Δ*ipcs*⁻ promastigotes *in vitro*. (A), growth; (B), PI exclusion (viability); (C), growth in the presence of 2 μM 3-keto-dihydrosphingosine; and (D), growth at pH 5.0 (MES buffer). All parasites were propagated in standard M199 culture media at 25º C. Lines tested are WT (●), Δ*ipcs*⁻ (○), or Δ*ipcs*⁻/+IPCS (▼).

Figure 5: Δ*ipcs*⁻ promastigotes are fully virulent in susceptible mice. 10^5 purified metacyclic parasites were inoculated into the footpad of Balb/C mice and the lesion size measured. Data from a representative experiment is shown, with the average and standard deviation for groups of 4 mice; simple linear regression determined significantly different slopes between groups ($p < 0.0001$); combined data from 4 separate experiments show similar trends and are provided in Fig. S4A.

Figure 6: ESI/MS analysis of lipids from purified amastigotes. (A,D), WT lesion amastigotes ; (B,E) purified Δ*ipcs*⁻ amastigotes (panels B,E); or (C,F), total infected footpad). Panels A-C show spectra using the positive ion mode (focusing here on sphingomyelin and PtEt species) and panels D-E using the negative ion mode and parent ion scanning (m/z = 241) (focusing on IPCs and inositol phospholipids) . Abbreviations: d16:1/18:0-PI-Cer, phosphoryl inositol N-stearoylhexadecesphing-4-enine (d16:1/18:0-IPC); d18:1/18:0-PICer, phosphoryl inositol N-stearoylsphingosine (d18:1/18:0-IPC); d18:o/18:0-PICer, phosphoryl inositol N-stearoylsphinganine (d18:0/18:0-IPC).

Figure 7: Relative abundance of amastigote SM and IPC. Purified lipids from WT amastigote preparations were spiked with the internal standards, 10 nmol N-Lauryl SM (positive ion mode, (panel A) and 2 nmol of dipalmitoyol phosphoinositol (negative ion mode, panel B) to compare the relative amounts of SM and IPC present in the same sample. This experiment was repeated a second time with similar results.

Figure 8. Characterization of the ceramide anchor of IPC species in WT promastigotes and amastigotes. (A), Summary of ESI/MS fragmentation steps and findings. The next panels show MS^3 analysis of the *m/z* 598 ceramide ion from amastigotes (B) or promastigotes (C). Fatty acid species are highlighted or circled in blue, while sphingoid-base-derived species (acid or ketene as described in the text) are highlighted or circled in red. Notably the deduced amastigote IPC anchor is the same as mammalian SM.

Figure 1

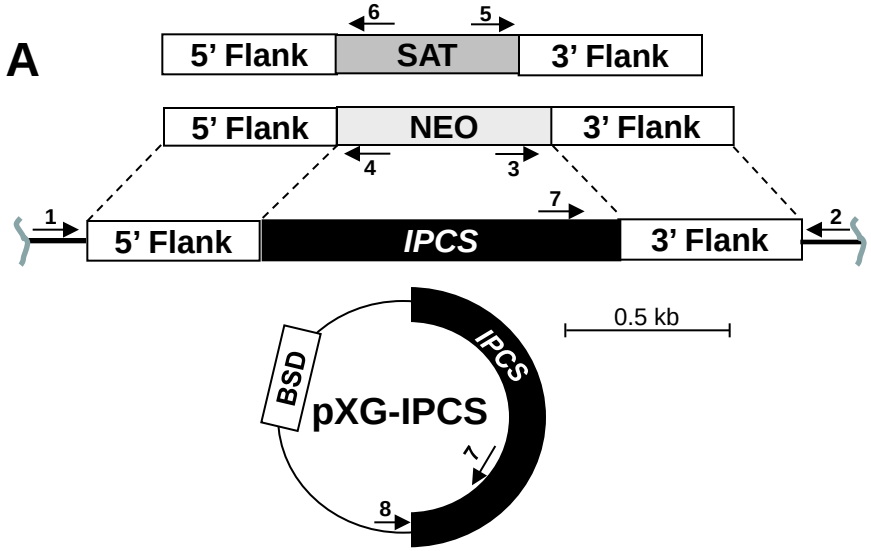
A
6
5
5' Flank
SAT
3' Flank
5' Flank
NEO
3' Flank
4
3
7
1
2
5' Flank
IPCS
3' Flank
0.5 kb
BSD
pXG-IPCS
IPCS
7
8

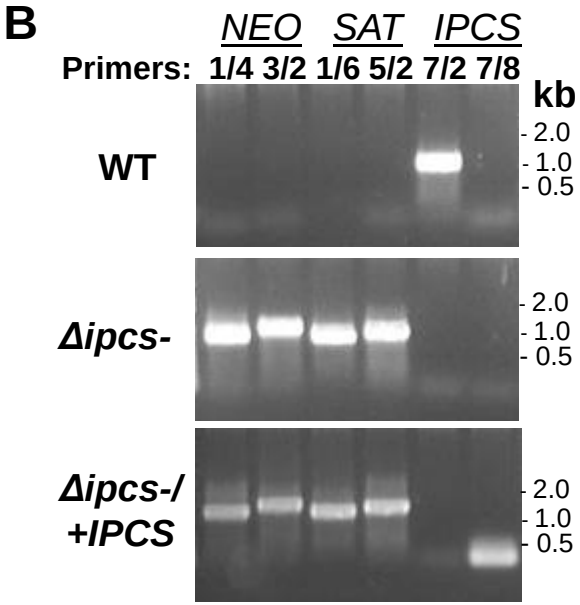
B
NEO SAT IPCS
Primers: 1/4 3/2 1/6 5/2 7/2 7/8
kb
WT
2.0
1.0
0.5
Δipcs-
2.0
1.0
0.5
Δipcs-/
+IPCS
2.0
1.0
0.5

Figure 2

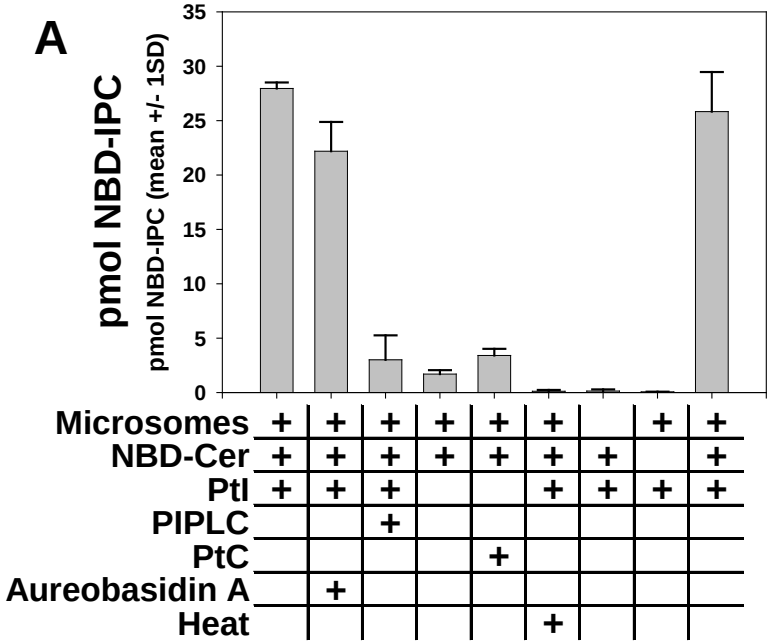
A
pmol NBD-IPC
pmol NBD-IPC (mean +/- 1SD)
35
30
25
20
15
10
5
0
Microsomes
NBD-Cer
PtI
PIPLC
PtC
Aureobasidin A
Heat

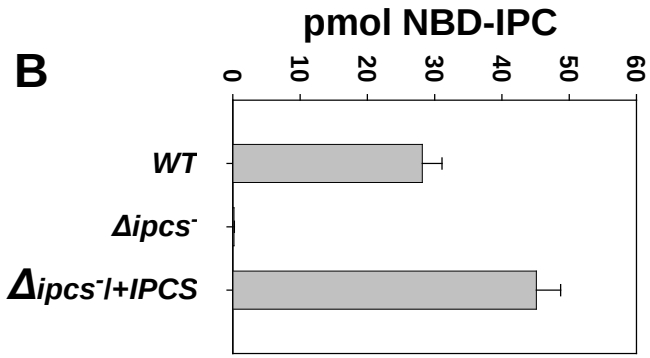
B
pmol NBD-IPC
0
10
20
30
40
50
60
WT
Δipcs-
Δipcs-/+IPCS

Figure 3

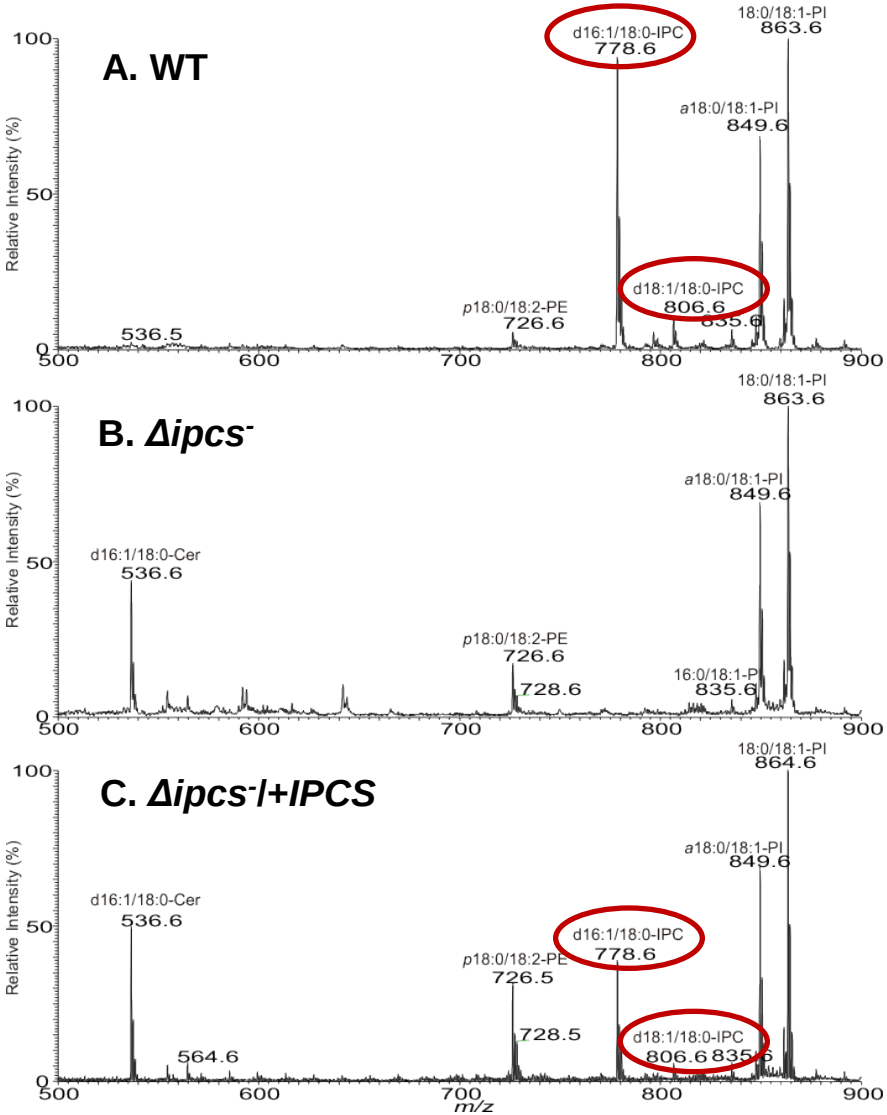
A. WT
B. Δipcs-
C. Δipcs-/+IPCS
Relative Intensity (%)
m/z
d16:1/18:0-IPC
778.6
18:0/18:1-PI
863.6
a18:0/18:1-PI
849.6
d18:1/18:0-IPC
806.6
835.6
p18:0/18:2-PE
726.6
536.5
d16:1/18:0-Cer
536.6
728.6
16:0/18:1-PI
835.6
864.6
726.5
728.5
564.6

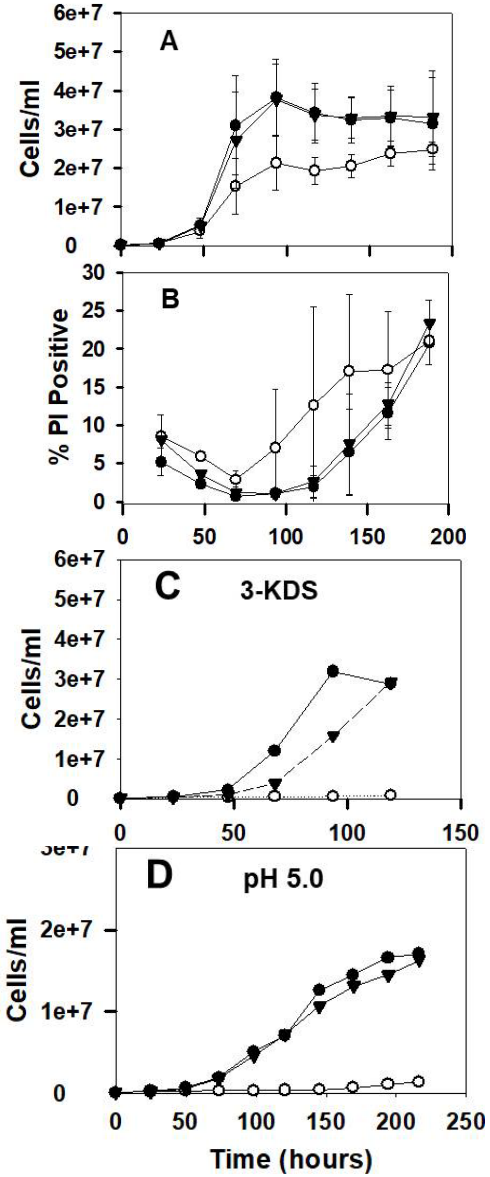
A
Cells/ml
6e+7
5e+7
4e+7
3e+7
2e+7
1e+7
0
B
% PI Positive
30
25
20
15
10
5
0
0
50
100
150
200
C
3-KDS
Cells/ml
6e+7
5e+7
4e+7
3e+7
2e+7
1e+7
0
0
50
100
150
D
pH 5.0
Cells/ml
2e+7
1e+7
0
0
50
100
150
200
250
Time (hours)

Figure 4

Figure 5. *Δipcs*⁻ remains virulent in animal infections

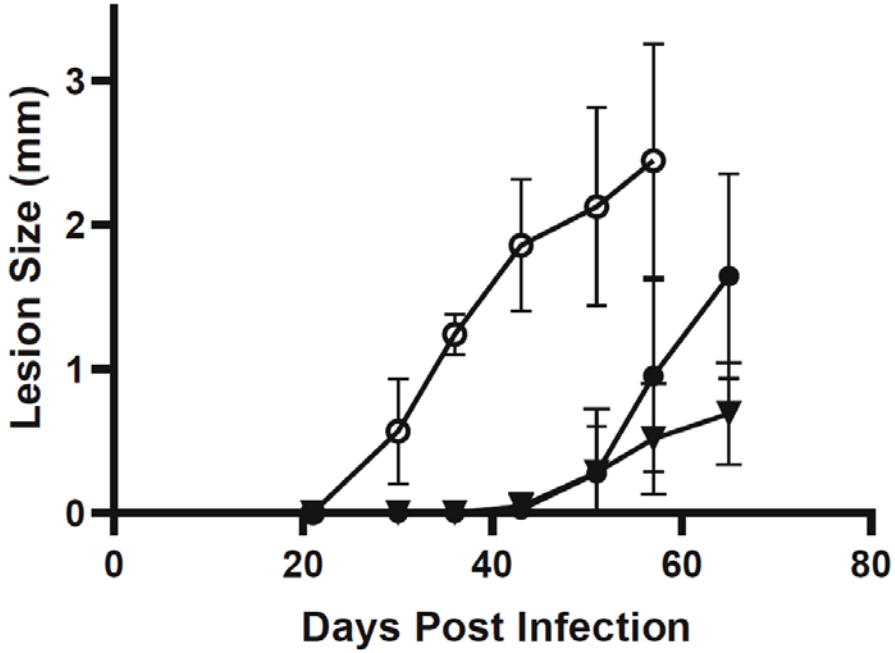

Figure 6

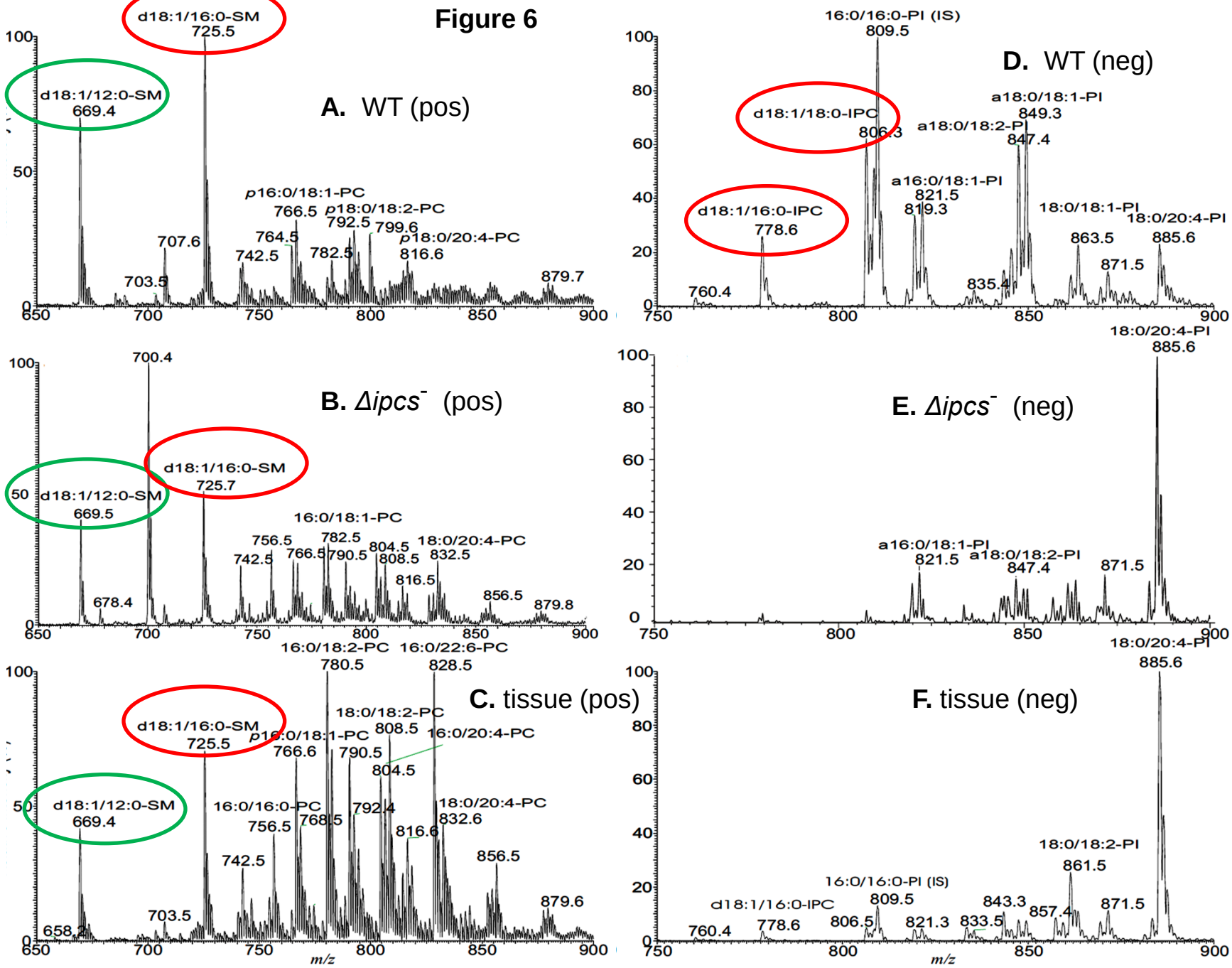
A. WT (pos)
d18:1/16:0-SM
725.5
d18:1/12:0-SM
669.4
707.6
703.5
742.5
764.5
766.5
p16:0/18:1-PC
782.5
792.5
p18:0/18:2-PC
799.6
p18:0/20:4-PC
816.6
879.7
B. Δipcs⁻ (pos)
700.4
d18:1/16:0-SM
725.7
d18:1/12:0-SM
669.5
678.4
16:0/18:1-PC
756.5
742.5
766.5
782.5
790.5
804.5
808.5
18:0/20:4-PC
832.5
816.5
856.5
879.8
C. tissue (pos)
16:0/18:2-PC
780.5
16:0/22:6-PC
828.5
18:0/18:2-PC
808.5
16:0/20:4-PC
d18:1/16:0-SM
725.5
p16:0/18:1-PC
766.6
790.5
804.5
d18:1/12:0-SM
669.4
16:0/16:0-PC
768.5
792.4
18:0/20:4-PC
832.6
756.5
816.6
742.5
856.5
879.6
703.5
658.2
m/z
D. WT (neg)
16:0/16:0-PI (IS)
809.5
d18:1/18:0-IPC
806.3
a18:0/18:1-PI
849.3
a18:0/18:2-PI
847.4
a16:0/18:1-PI
821.5
819.3
d18:1/16:0-IPC
778.6
18:0/18:1-PI
18:0/20:4-PI
863.5
885.6
871.5
835.4
760.4
E. Δipcs⁻ (neg)
18:0/20:4-PI
885.6
a16:0/18:1-PI
821.5
a18:0/18:2-PI
847.4
871.5
F. tissue (neg)
885.6
18:0/18:2-PI
861.5
16:0/16:0-PI (IS)
809.5
d18:1/16:0-IPC
843.3
857.4
871.5
760.4
778.6
806.5
821.3
833.5
m/z

Figure 7

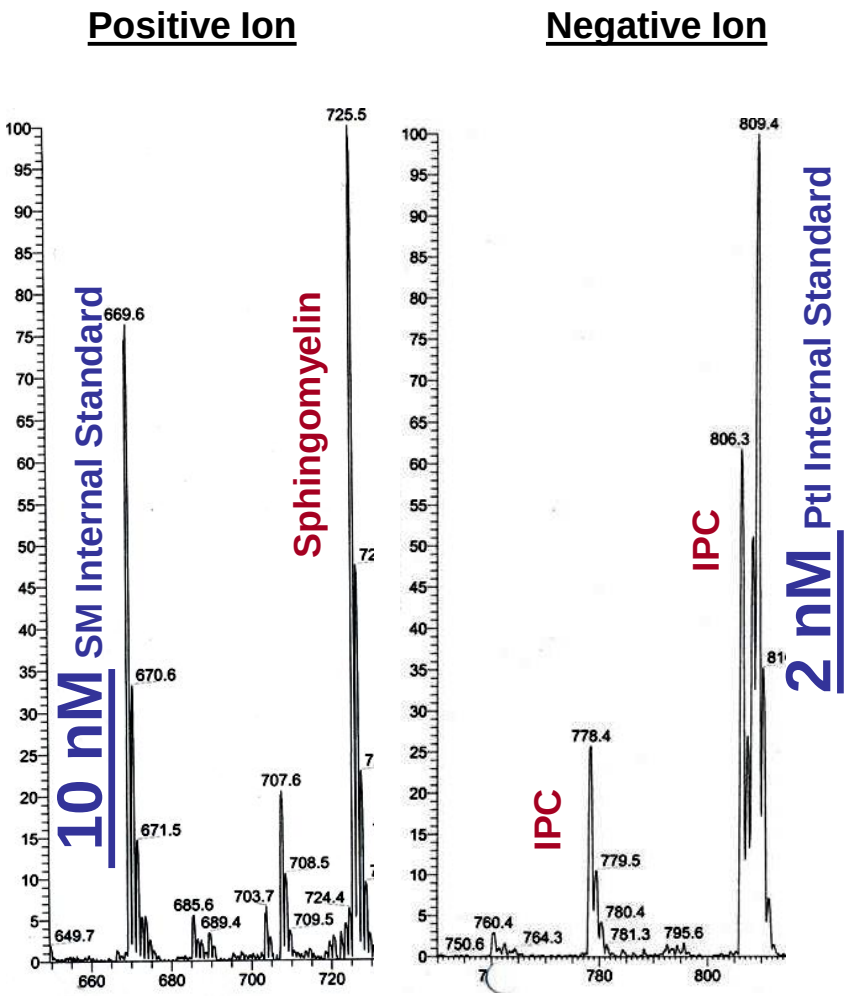
Positive Ion
Negative Ion
10 nM SM Internal Standard
Sphingomyelin
669.6
670.6
671.5
649.7
685.6
689.4
703.7
707.6
708.5
709.5
724.4
725.5
IPC
IPC
2 nM PtI Internal Standard
809.4
806.3
778.4
779.5
780.4
781.3
795.6
760.4
764.3
750.6

Figure 8

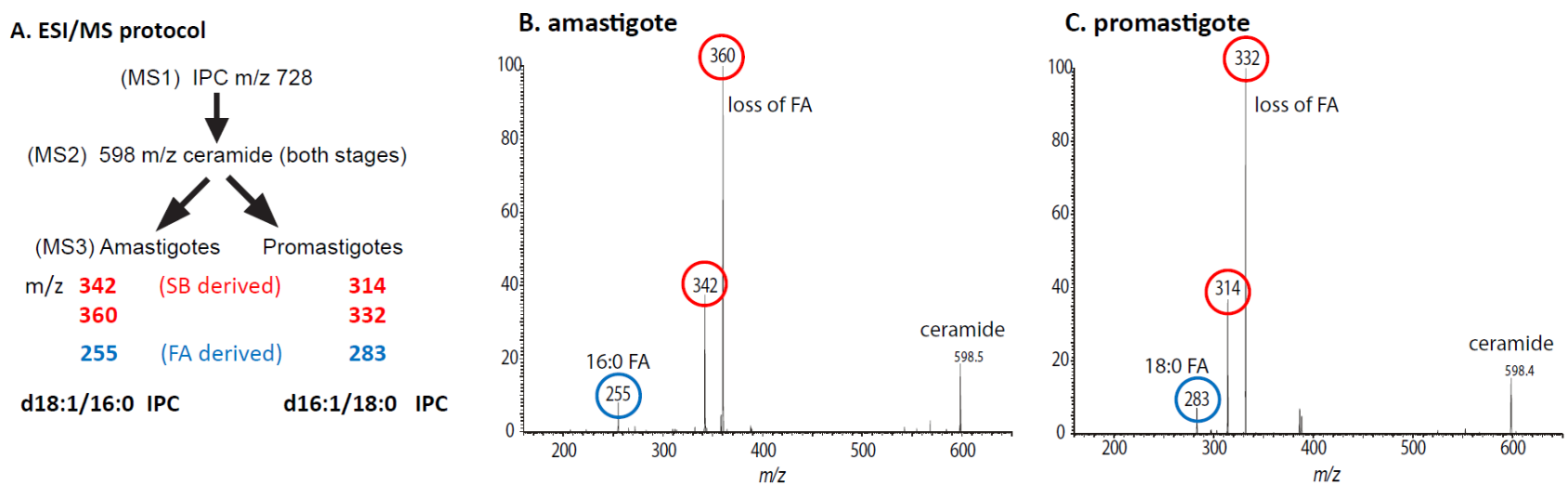
A. ESI/MS protocol
(MS1) IPC m/z 728
(MS2) 598 m/z ceramide (both stages)
(MS3) Amastigotes
Promastigotes
m/z 342 (SB derived) 314
360 332
255 (FA derived) 283
d18:1/16:0 IPC
d16:1/18:0 IPC
B. amastigote
360
loss of FA
342
16:0 FA
255
ceramide
598.5
m/z
C. promastigote
332
loss of FA
314
18:0 FA
283
ceramide
598.4
m/z

Supporting information.

"Inositol Phosphorlyceramide Synthase null *Leishmania major* (Δ*ipcs*⁻) are viable and virulent in animal infections where salvage of host sphingomyelin predominates"

F. Matthew Kuhlmann, Phillip Key, Suzanne Hickerson, John Turk, Fong-Fu Hsu, and Stephen M. Beverley

Materials included.

Supplemental Table 1. Oligonucleotides used

Supplemental Table 2. Δ*ipcs*⁻ is strongly inhibited below pH 5.5

Supplemental Figure 1. Representative TLC data relevant to enzymatic characterization of IPCS activity from purified microsomes, and its absence in Δ*ipcs*⁻ promastigotes.

Supplemental Figure 2. Phenotypic characterization of WT and Δ*ipcs*⁻ mutant *L. major* propagated in M199 medium *in vitro*.

Supplemental Figure 3. Accumulation of phytoceramide in Δ*ipcs*⁻ parasites grown in the presence of phytosphingosine.

Supplemental Figure 4. *Δipcs*- remains highly virulent in animal infections

Supplemental Table 1. Oligonucleotides used in this work.

Primer number	Sequence (5'-3')	Purpose
SMB2586		forward primer to amplify *NEO* marker
SMB2587		reverse primer to amplify *NEO* marker
SMB2588		forward primer to amplify *SAT* marker
SMB2589		reverse primer to amplify SAT marker
SMB2590		forward primer to amplify 5' flanking region of *IPCS*
SMB2591		reverse primer to amplify 5' flanking region of *IPCS*
SMB2592		forward primer to amplify 3' flanking region of *IPCS*
SMB2593		reverse primer to amplify 3' flanking region of *IPCS*
SMB3259		forward primer to amplify *IPCS*
SMB3260		reverse primer to amplify *IPCS*

Supplemental Table 2.

Growth of *Δipcs⁻ in vitro* is strongly inhibited below pH 5.5

The doubling time (hr) and standard deviations (n=??) of WT, *Δipcs⁻* or *Δipcs⁻/+IPC* with the indicated pH and overlapping buffers is shown.

Buffer	pH	WT	*Δipcs⁻*	*Δipcs⁻/+IPC*
Citrate	5	19.7 ± 0.3	59.9 ± 18.6	20.8 ± 2.1
	5.5	10.8 ± 0.0	15.3 ± 3.7	11.3 ± 0.9
	6	9.5 ± 0.1	12.3 ± 1.8	10.1 ± 0.4
MES	5	66.8 ± 25.6	390.0 ± 119.3	35.0 ± 29.1
	5.5	20.1 ± 11.0	22.2 ± 9.9	46.6 ± 52.5
	6	8.8 ± 0.4	8.0 ± 4.2	9.2 ± 0.5
HEPES	6.8	8.4 ± 0.2	10.7 ± 0.1	9.3 ± 0.4

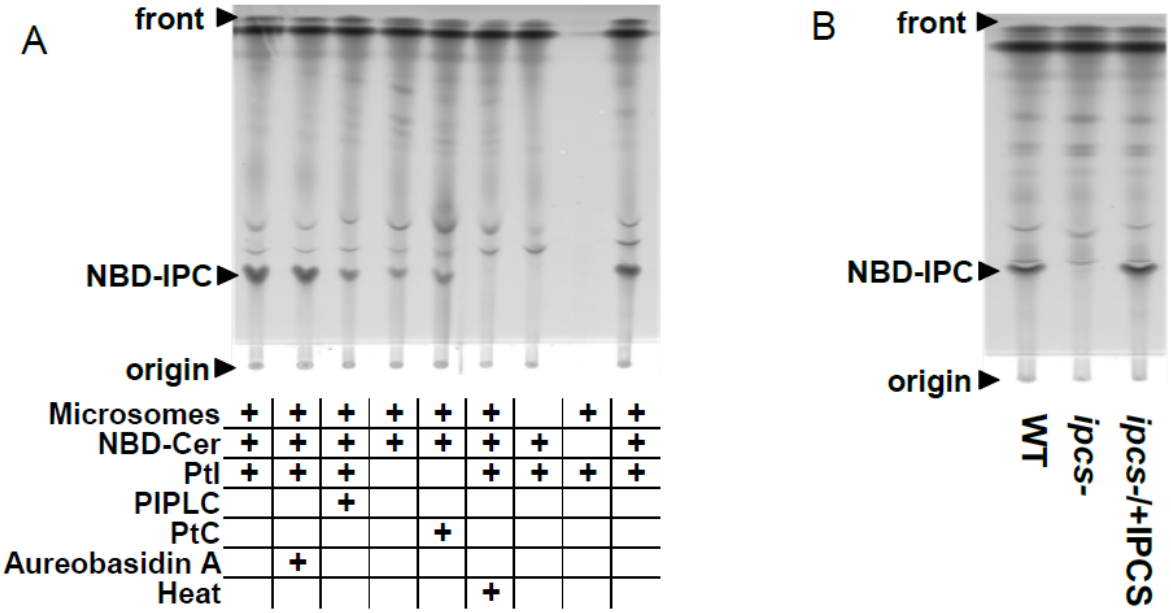

Figure S1: **Enzymatic characterization of IPCS activity from purified microsomes, and its absence in Δ*ipcs*⁻ promastigotes.**

The figure displays representative TLC separations used for the quantitative plots shown in Fig. 2.

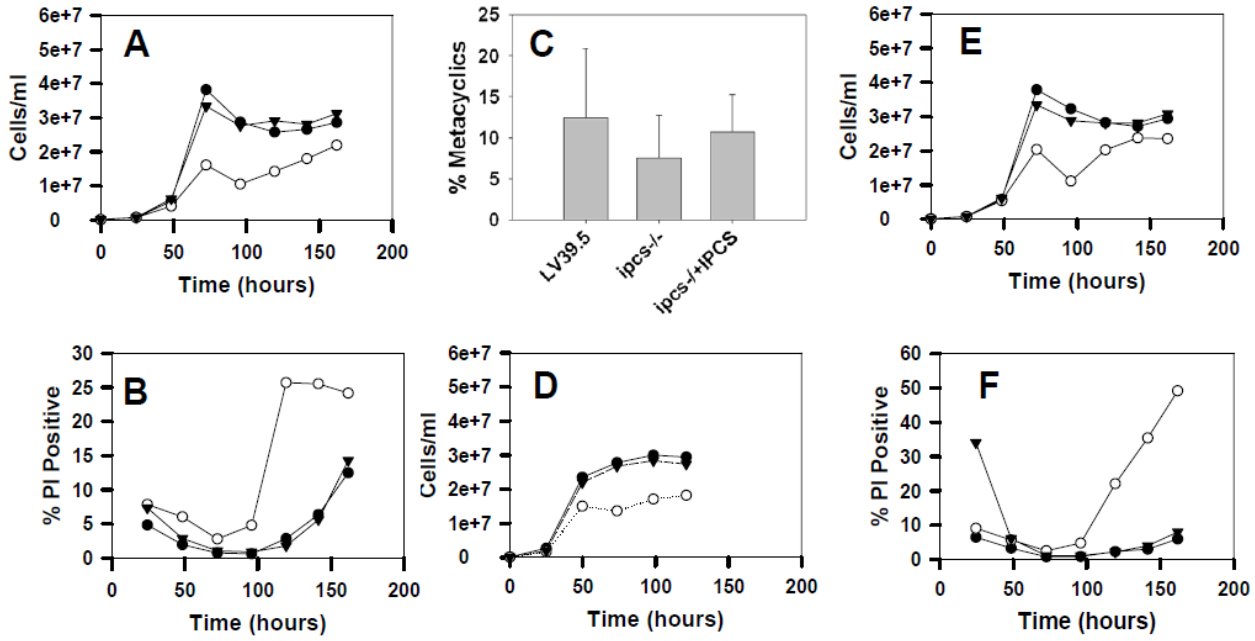

Figure S2: Phenotypic characterization of WT and Δ*ipcs*⁻ mutant *L. major* propagated in M199 medium *in vitro*.

(A,B), Growth and viability of parasites grown in 500 µM EtN. (C), Percent metacyclic observed at day 2 in stationary phase. (D), Growth of parasites at 33°C (at 37º all lines died). (E.F), growth and viability of parasites supplemented daily with 2 µM DAG.

Symbols are WT (●), Δ*ipcs*⁻ (○), or Δ*ipcs*⁻/+*IPCS* (▼).

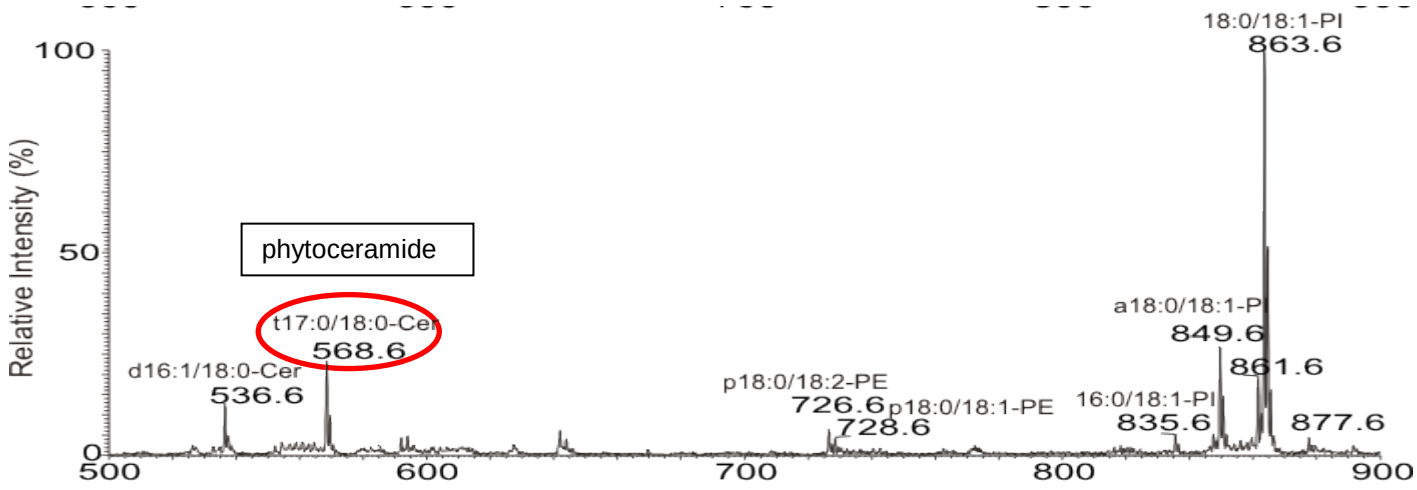

Figure S3: Accumulation of phytoceramide in Δ*ipcs*⁻ parasites grown in the presence of phytosphingosine.

The ESI/MS (negative ion mode) spectra obtained using purified lipids is shown. *In vitro* cultures of Δ*ipcs*⁻ parasites were inoculated at 1 x 10^6 cells/ml in M199 media containing 8 µM C17-phytosphingosine and grown 16 hr. The peak corresponding to phytoceramide (m/z 568) is circled. Nomenclature for individual lipid species is provided in the legends of Fig. 3 and Fig. 6.

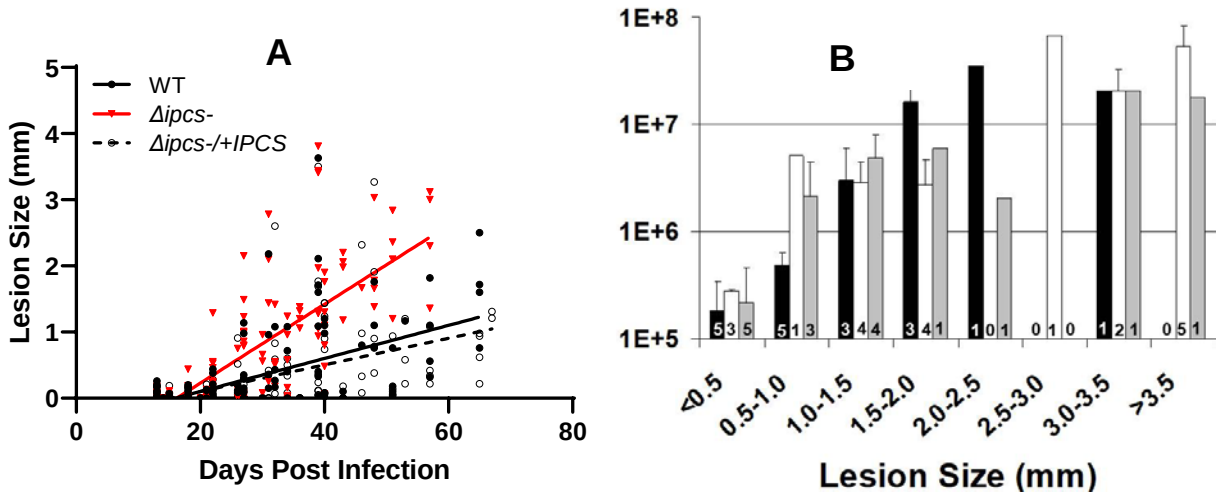

Figure S4. *Δipcs*- remains highly virulent in animal infections.

(A) Collected data from four independent experiments with 4-8 mice/group are plotted (a representative individual experiment is shown in Fig. 5). The lines shown were obtained by simple linear regression showing significant differences between *Δipcs*⁻ and WT or *Δipcs*⁻ /+*IPCS* ($p < 0.0001$).

(B) Limiting dilution assays show a similar relationship between lesion size and parasite numbers in WT and mutant L. major. At various time points post-infection, lesions were excised and parasite numbers determined by limiting dilution. As not every experiment yielded lesions of a given size at the times measured for comparison, the small numbers within the bars denote the number of lesions, and the standard deviation is shown when possible. Parasite lines were WT (black bar), *Δipcs*- (white bar), and *Δipcs-/+IPCS* (gray bar) lesions.